LANGMUIR

Article

pubs.acs.org/Langmuir

Facile Assembly of Large-Area 2D Microgel Colloidal Crystals Using Charge-Reversible Substrates

Junying Weng,[†] Xiaoyun Li,[†] Ying Guan,*[,†] X. X. Zhu,[‡] and Yongjun Zhang*[,†]

[†]Key Laboratory of Functional Polymer Materials and State Key Laboratory of Medicinal Chemical Biology, The Co-Innovation Center of Chemistry and Chemical Engineering of Tianjin, Institute of Polymer Chemistry, College of Chemistry, Nankai University, Tianjin 300071, China

[‡]Department of Chemistry, Université de Montréal, C. P. 6128, Succursale Centre-ville, Montreal, Québec H3C 3J7, Canada

Supporting Information

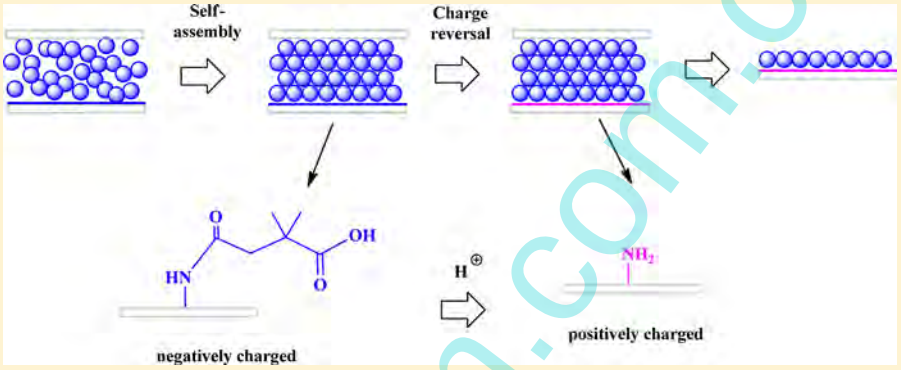

ABSTRACT: 2D colloidal crystals (CCs) have important applications; however, the fabrication of large-area, high-quality 2D CCs is still far from being trivial, and the fabrication of 2D microgel CCs is even harder. Here, we have demonstrated that they can be facilely fabricated using charge-reversible substrates. The charge-reversible substrates were prepared by modification with amino groups. The amino groups were then protected by amidation with 2,2-dimethylsuccinic anhydride. At acidic pH, the surface charge of the modified substrate will change from negative to positive as a result of the hydrolysis of the amide bonds and the regeneration of the amino groups. 2D microgel CCs can be simply fabricated by applying a concentrated microgel dispersion on the modified substrate. The negatively charged surface of the substrate allows the negatively charged microgel spheres, especially those close to the substrate, to self-assemble into 3D CCs. With the gradual hydrolysis of the amide bonds and the charge reversal of the substrate, the first 111 plane of the 3D assembly is fixed in situ on the substrate. The resulting 2D CC has a high degree of ordering because of the high quality of the parent 3D microgel CC. Because large-area 3D microgel CCs can be facilely fabricated, this method allows for the fabrication of 2D CCs of any size. Nonplanar substrates can also be used. In addition, the interparticle distance of the 2D array can be tuned by the concentration of the microgel dispersion. Besides rigid substrates (such as glass slides, quartz slides, and silicon wafers), flexible polymer films, including polyethylene terephthalate and poly(vinyl chloride) films, were also successfully used as substrates for the fabrication of 2D microgel CCs.

INTRODUCTION

2D colloidal crystals (CCs) are ordered monolayer arrays of colloidal microspheres.[1−4] Like their 3D analogues, they have found important applications in 2D photonic crystals[5] and sensors.[6−9] Particularly, the fabrication of 2D CCs provides a simple, fast, and inexpensive method for surface patterning.[1−4] More importantly, they could be further used as masks or templates in colloidal lithography: a facile, inexpensive, and repeatable nanofabrication technique for 2D arrays of nanostructures with novel functions.[1−4] However, the reliable assembly of large-area, high-quality 2D CCs is still far from being trivial, even though it has been subjected to intense research for 3 decades.[4]

Usually, 2D CCs are assembled from hard colloids, such as polystyrene,[6,8−14] PMMA,[15,16] and SiO_2.[14,17,18] Soft hydrogel colloids, for example, poly(*N*-isopropylacrylamide) (PNIPAM) microgel spheres, have also been used to assemble 2D CCs. Like 2D CCs of hard colloids, 2D microgel CCs have also found important application in various areas, for example, in colloidal lithography.[19−21] Recently, using the 2D microgel CC as a lithographic mask, Isa et al.[21] have synthesized large-area arrays of vertically aligned silicon nanowires by metal-assisted chemical etching. As a building block for the 2D CC, an intriguing advantage of microgel spheres over hard colloids may be that the former could respond to external stimuli and thus change their size and properties.[22,23] This makes them quite

Received: September 12, 2016
Revised: October 27, 2016
Published: November 4, 2016

DOI: 10.1021/acs.langmuir.6b03359
Langmuir 2016, 32, 12876−12884

Scheme 1. (A) Preparation of Charge-Reversible Substrates (Glass Slide as an Example) and (B) Fabrication of a 2D Microgel CCs on a Charge-Reversible Substrate[a]

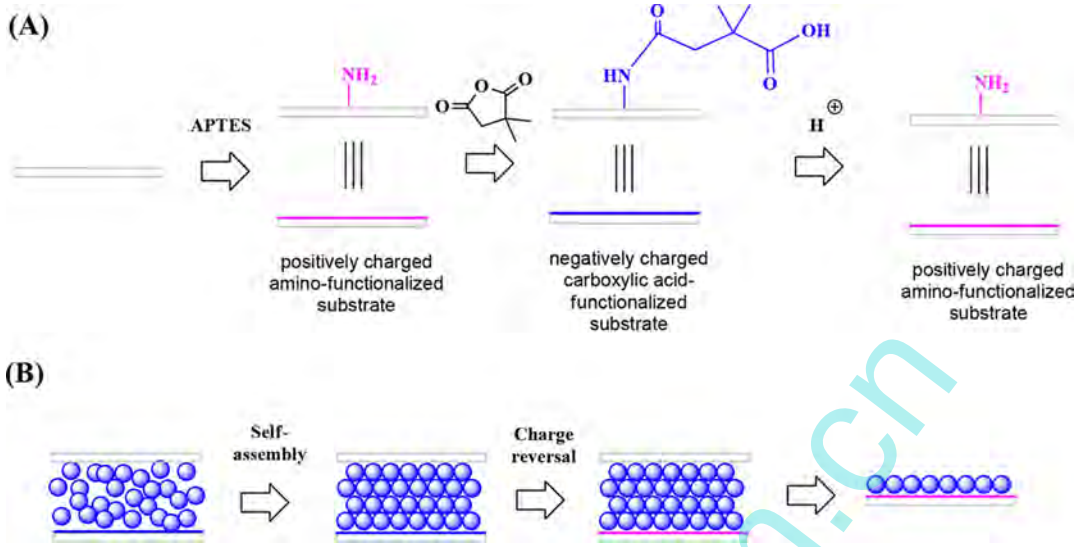

[a](A) The substrate was first treated with APTES to introduce amino groups. The amino groups were then protected by reaction with 2,2-dimethylsuccinic anhydride. The resulting amides are hydrolyzable. Their hydrolysis in acidic solutions results in the regeneration of amino groups and surface charge reversal of the substrate. (B) A 3D microgel CC was first assembled on the substrate. With the spontaneous charge reversal of the substrate during aging, the first 111 plane was fixed in situ onto the substrate via electrostatic interaction. The removal of the unbound spheres gives a 2D microgel CC.

suitable for the creation of functional 2D CCs, a future direction for the study of 2D CCs, as suggested by Vogel et al.[4] As an example, Xu et al.[24] demonstrated that a 2D microgel CC could be used to control the attachment and growth of cells seeded on the monolayer because they are thermosensitive.

Like 2D CCs of hard colloids, the assembly of high-quality 2D microgel CCs is not easy. Presently, 2D microgel CCs are fabricated via dip-coating,[19,25] solvent evaporation,[20,23,26−28] and interfacial assembly.[21,29−31] These methods were originally developed for the fabrication of 2D CCs from hard colloids;[1−4] therefore, 2D microgel CCs usually suffer from the same problems as 2D CCs of hard colloids. The size of the resulting arrays is usually small.[6,20,26] Many of the methods, for example, the spin-coating method,[29] allow for only the use of planar substrates. Some methods, for example, the one developed by Isa et al.,[30] require certain specific equipment (Langmuir trough). In addition, the 2D ordering can easily be lost upon drying or transferring because of their soft nature. Therefore, it is more difficult to assemble microgel spheres than hard colloids.[24]

We recently proposed a new strategy for the fabrication of high-quality, large-area 2D CCs of microgel spheres, in which the microgel spheres were first assembled into 3D CCs, followed by in situ fixing of the first 111 plane of the 3D assembly.[32,33] Taking advantage of the easy assembly of large-area, high-quality 3D microgel CCs,[34−42] large-area, high-quality 2D microgel CCs can be facilely fabricated. Besides planar substrates, 2D microgel CCs can also be fabricated on nonplanar substrates. In addition, the interparticle distance can be facilely tuned.[32,33] In this strategy, the key is the in situ fixing of the microgel spheres onto the substrate. Previously, we used a photochemical reaction between the substrate and the microgel spheres to fix the microgel spheres,[32,33] which requires UV irradiation to initiate the reaction. Here, we demonstrated that by using a charge-reversible substrate, the microgel spheres could also be fixed in situ as a result of the charge reversal of the substrate surface (Scheme 1). The reaction occurs spontaneously and the UV-irradiation step is no longer required, making the method extremely simple. However, large-area, high-quality 2D microgel CCs can still be fabricated on both planar and nonplanar substrates.

EXPERIMENTAL SECTION

Materials. *N*-Isopropylacrylamide (NIPAM) and *N*,*N*′-methylenebis(acrylamide) (BIS) were purchased from Alfa Aesar. Acrylic acid (AA) and 3-aminopropyltriethoxysilane (APTES) were purchased from Acros. Sodium dodecyl sulfate (SDS) was purchased from Sigma-Aldrich. Potassium persulfate (KPS), 1,6-diaminohexane, 2,2-dimethylsuccinic anhydride, tetraethyl orthosilicate (TEOS), and ethylenediamine were purchased from local providers. NIPAM was purified by recrystallization from hexane/acetone mixture and dried in a vacuum. AA was distilled under reduced pressure. Toluene was dried over dehydrated $CaCl_2$ and distilled with sodium/benzophenone before use.

Microgel Synthesis. Poly(*N*-isopropylacrylamide-*co*-acrylic acid) (P(NIPAM-AA)) copolymer microgels with different sizes were synthesized via free-radical precipitation polymerization. For the 700 and 880 nm microgels, NIPAM, AA, and BIS were dissolved in 95 mL of water. The total amount of the monomers in feed was 0.015 mol, and their molar ratio, NIPAM/AA/BIS, was 88.45:10:1.55. For 700 nm microgel, 0.01 g of SDS was also added. The solution was purged with nitrogen and heated to 70 °C. After 1 h, 5 mL of 0.06 M KPS solution was added to initiate the polymerization. The reaction was allowed to process for 4 h. The resulting microgels were purified by three successive centrifugation (12 000*g* for 1 h)−decantation−redispersion cycles.

The 1030 and 1430 nm microgels were synthesized by adding a shell to a core microgel as described by Jones and Lyon.[43] Similarly, NIPAM, AA, and BIS were dissolved in 95 mL of water. The total amount of the monomers was again 0.015 mol, and their molar ratio, NIPAM/AA/BIS, was 88.9:10:1.1 for 1030 nm microgel, and 88.6:10:1.4 for the 1430 nm microgel. The solution was purged with nitrogen and heated to 70 °C. After 1 h, 5 mL of 0.06 M KPS solution was added to initiate the polymerization. The reaction was allowed to process for 4 h. Then, a preheated shell solution with the same

DOI: 10.1021/acs.langmuir.6b03359
Langmuir 2016, 32, 12876−12884

composition was added. After purging with N_2 for another 30 min, 5 mL of 0.06 M APS solution was added. The reaction was allowed to process for additional 4 h. The resulting microgels were again purified by three successive centrifugation, decantation, and redispersion cycles. The microgels were named according to their hydrodynamic diameter (D_h) at 20 °C.

Synthesis and Surface Modification of Silica Nanoparticles. To synthesize silica nanoparticles, 10 mL of TEOS, 160 mL of ethanol, and 40 mL of deionized (DI) water were mixed. After stirring for half an hour, 2.4 mL of concentrated ammonium hydroxide was added. The sol−gel reaction was allowed to process for 4 h. The resulting particles were separated by centrifugation and purified by washing with DI water and ethanol, each for three times. Finally, the particles were dried at 60 °C overnight. The hydrodynamic diameter (D_h) of the particles was measured to be ∼220 nm.

To functionalize with amino groups, 1 g of the silica particles was dispersed in 80 mL of anhydrous toluene while purging with N_2. After heated to 70 °C, 1 mL of APTES was added. The reaction was allowed to process for 4 h. The resultant amino-functionalized particles were separated by centrifugation, followed by washing with acetone and tetrahydrofuran (THF), each for three times, and overnight drying in vacuum at 30 °C. The particles were then amidated as follows.[44] First, 0.5 g of amino-functionalized particles was dispersed into a mixture of 50 mL of THF, 5 mL of pyridine, and 2 g of 2,2-dimethylsuccinic anhydride. The solution was then heated to 50 °C while purging with N_2. The reaction was allowed to process for 8 h. Similarly, the resultant carboxylic acid-functionalized particles were separated by centrifugation, followed by washing with acetone, THF, water, and overnight drying in vacuum at 30 °C.

Surface Modification of Glass Slides. Glass slides were cut into 1.5 × 2.5 cm^2 pieces and cleaned in a freshly prepared piranha solution (1:3 v/v H_2O_2−H_2SO_4 mixture) (**caution**: this solution is extremely corrosive) for 6 h, rinsed thoroughly with DI water, and dried in a stream of nitrogen. They were then immersed in 1 wt % anhydrous toluene solution of APTES for 4 h at room temperature, sonicated twice in toluene, each for 10 min, and dried in a stream of nitrogen.[45] The amino-functionalized substrates were then incubated in anhydrous THF containing 10 mg/mL 2,2-dimethylsuccinic anhydride and 5% triethylamine (TEA) for 10 h.[46] After rinsing with methanol and DI water, the substrates were dried in a stream of nitrogen. Silicon wafers and quartz slides were modified in the same way.

Surface Modification of Polyethylene Terephthalate Films. Polyethylene terephthalate (PET) films were first aminolyzed according to refs 47 and 48. The films were first immersed in an alcohol/water (1:1, v/v) solution for 4 h to remove any oily dirt on the surface. They were then incubated in propyl alcohol containing 0.06 g/mL of 1,6-diaminohexane at 30 °C for 4 h. After washing with water, the films were dried at 37 °C for 24 h. Subsequently, the amino-functionalized films were immersed in propyl alcohol containing 10 mg/mL of 2,2-dimethylsuccinic anhydride and 5% TEA at 30 °C for 12 h. After washing with propyl alcohol, they were dried at 37 °C for 24 h.

Surface Modification of Poly(vinyl chloride) Films. According to ref 49, amination of poly(vinyl chloride) (PVC) films was performed by immersing the films in 80% aqueous solution of ethylenediamine at 80 °C for 2 h. They were then washed with copious amounts of DI water and dried in a stream of nitrogen. Similarly, the amino-functionalized PVC films were immersed in propyl alcohol containing 10 mg/mL of 2,2-dimethylsuccinic anhydride and 5% TEA at 30 °C for 12 h. After washing with propyl alcohol, they were dried at 37 °C for 24 h.

Fabrication of 2D Microgel Arrays. The microgel dispersions were first concentrated by centrifugation. They were then loaded into cells composed of a glass slide and a surface-modified substrate (glass slide, silicon wafer, quartz slide, or PET or PVC film) separated by two layers of Parafilm. The dispersions were allowed to age at ∼22 °C for 5 days. The cells were then opened, and the substrates were rinsed thoroughly in flowing DI water. They were then dried in a stream of nitrogen.

Characterization. The zeta potential of the silica nanoparticles was determined on a Zetasizer Nano ZS90. The size and size distribution of microgel particles were determined using dynamic light scattering with a Brookhaven 90Plus laser particle size analyzer. All measurements were carried out at a scattering angle of 90°. The sample temperature was controlled with a built-in Peltier temperature controller. Atomic force microscopy (AFM) of the 2D arrays was performed on a CSPM5500 scanning probe microscope in a tapping mode (Benyuan, China). The optical images were acquired on a Leica TCS SP8 confocal microscope in a bright-field mode.

RESULTS AND DISCUSSION

Microgel Synthesis and Substrate Modification. As schematically shown in Scheme 1, the strategy used here exploits the ability of the microgel spheres to self-assemble into a highly ordered 3D CC[36,41,42] and the ability of the substrate to change its surface charge from negative to positive. In this way, the negatively charged microgel spheres close to the substrate, which form the 111 plane of the 3D CC, will be fixed in situ on the substrate.

The PNIPAM microgel spheres used for the assembly were synthesized by free-radical precipitation polymerization. All of the microgels exhibit a narrow size distribution. Their thermosensitive behaviors are shown in Figure S1. They all bear negative charges, as indicated by their negative zeta potentials (Table S1).

We first used glass slides as a substrate to fabricate the 2D CCs. To make them charge-reversible, the slides were first modified with amino groups to create a positively charged surface. The surface-bound amino groups then reacted with 2,2-dimethylsuccinic anhydride. The resulting surface would be covered with carboxylic acid groups and hence negatively charged (Scheme 1A). When immersed in an acidic solution, with the hydrolysis of the amides, the amino groups will be regenerated, and therefore, the surface charge will be reversed to be positive (Scheme 1A).

It was previously reported that amides with neighboring carboxylic acid groups, as the one used here, exhibit pH-dependent hydrolysis.[50] They are stable at neutral pH but hydrolyze and regenerate the amino groups at a low pH. Therefore, they were widely used to design charge-reversible polymers.[50−54] To confirm that the surface charge of the glass slide could be reversed, silica nanoparticles, with a surface chemistry similar to glass slides, were used as a model system. Similar to glass slides, the silica nanoparticles were surface-modified by first reacting with APTES to introduce surface amino groups and then reacting with 2,2-dimethylsuccinic anhydride to convert amino groups to carboxylic acid groups (Scheme S1). They were then dispersed in an acidic aqueous solution. The pH and temperature of the solution were adjusted to be the same with the microgel dispersions used below (pH = 3.5, T = 22 °C). At the beginning, the particles exhibit a negative zeta potential (−6.5 mV), suggesting that they bear negative charges (mainly because of the surface carboxylate groups). As shown in Figure 1, the value of zeta potential of the particles decreases with time and becomes zero after about 24 h incubation. Thereafter, the zeta potential turns to be positive and continues increasing with time. A maximum value of +25 mV was finally reached after 5 day incubation. The result clearly suggests that the surface amide bonds hydrolyze in acidic solutions, resulting in charge reversal of the nanoparticles. It is believed that when immersing the surface-modified glass slides in an acid solution, the same hydrolysis-induced charge reversal will take place too.

DOI: 10.1021/acs.langmuir.6b03359
Langmuir 2016, 32, 12876−12884

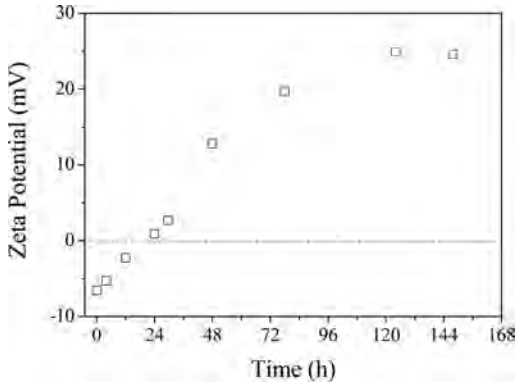

Figure 1. Zeta potential of surface-modified silica particles as a function of time at pH 3.5 and 22 °C. The particles were modified sequentially with APTES and 2,2-dimethylsuccinic anhydride.

Fabrication of 2D Microgel CCs. As shown in Scheme 1, 2D microgel CCs were simply fabricated by loading concentrated microgel dispersion in a cell composed of two glass slides, one of which was surface-modified. After aging for a short time, the samples become iridescently colored, indicating the successful assembly of a 3D microgel CC (see the typical image shown in Figure S2).[35,36,38,39] Examination with an optical microscope reveals that the microgel spheres are arranged into a hexagonally close-packed crystalline array. Figure 2A shows a typical image, which was taken from the

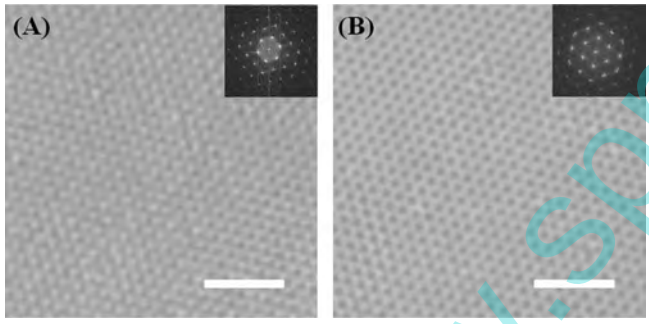

Figure 2. Optical micrograph of the interior region (A) and the layer close to the substrate (B) of a 3D CC assembled from the 1030 nm microgel (the concentration was 3.32 wt %). The insets show the FFT of the images. Scale bars: 5 μm.

interior part of the crystal. The fast Fourier transformation (FFT) of the image confirms again a structure with long-range order and hexagonal symmetry.[35] More importantly, as shown in Figure 2B, the microgel spheres close to the substrate are also arranged into a hexagonally close-packed crystalline array, just like the particles in the interior region. As Debord and Lyon[56] had pointed out, these spheres actually form the first 111 plane of the face-centered cubic (fcc) lattice of the 3D CC. In addition, compared with the 111 planes in the interior region, the degree of order of the first 111 plane is not reduced, which is in agreement with the previous observation by Alsayed et al.[57]

The dispersion was allowed to age for a period of 5 days. During this period, with the hydrolysis of the amide bonds as shown in Scheme 1, which is triggered by the acidic environment provided by the microgel dispersion (the pH of the microgel dispersions was measured to be ~3.5), the surface charge of the substrate will gradually change from negative to positive. Consequently, the microgel spheres close to the substrate will be fixed onto the substrate because of the electrostatic interaction between the negative charges on the microgel spheres and the positive charges on the substrate. A 5 day aging period was chosen because the hydrolysis of the amide bonds completes in about 5 days, as shown in Figure 1. The unbound microgel spheres were then washed away, leaving a 2D microgel array on the substrate.

Figure 3 shows the AFM and optical microscopy images of the 2D arrays assembled from four microgels. One can observe that all arrays exhibit a highly ordered structure, suggesting that the ordered structure of the microgel array close to the substrate was maintained because the microgel spheres were fixed onto the substrate in situ. The result also suggests that washing in water and drying in the air do not disturb the preformed-ordered structure. In other words, the electrostatic interaction between the microgel spheres and the substrate is high enough for the microgel spheres to resist the disturbance.

As controls, 2D microgel arrays were also fabricated using substrates with a different surface chemistry. In the first control, bare (unmodified) glass slides were used. Similarly, 3D microgel CCs were first assembled on the substrate, and 5 days later, the unbound spheres were removed by washing with water. The AFM image of the resulting 2D array is shown in Figure 4A. One can observe that many microgel spheres were missing, suggesting that they were washed away because of the relatively weak interaction between the particles and the substrate.[33] To fabricate the highly ordered array as shown in Figure 3, the interaction between the particles and the substrate must be strengthened.

In the second control, the substrate was only modified with APTES, but not further with 2,2-dimethylsuccinic anhydride, that is, the surface amino groups were not converted to carboxylic acid groups. When the substrate was used, it could be fully covered by microgel spheres, as shown in Figure 4B, which can be attributed to an enhanced interaction between the particles and the substrate because of the introduction of amino groups. However, the spheres were not arranged in an ordered structure. The reason should be that when the microgel dispersion was added, the negatively charged spheres were immediately stuck onto the positively charged substrate. In addition, the strong attractive interaction between the spheres and the substrate prevents the spheres from self-assembling into an ordered structure. As a result, a disordered array, instead of an ordered one, was obtained. The results highlight the importance of the protection of the amino groups with hydrolyzable amides. At the initial stage of the aging, it allows the microgel spheres close to the substrate to self-assemble into a highly ordered structure. Meanwhile, it allows the regeneration of the amino groups at the later stage and thus strengthening the interaction between the microgel spheres and the substrate.

The microscopy images shown in Figure 3 indicate that the resulting 2D arrays are highly ordered. The ordering of the arrays was also checked using other methods. Laser diffraction is a convenient method for this purpose.[58,59] When illuminated with a monochromatic laser light, a perfect hexagonal array will give a diffraction pattern composed of a set of distinct spots with six-fold symmetry.[59] Different places of the same sample were checked, and the same diffraction pattern was obtained. Many previously reported 2D CCs display a diffraction pattern of a sharp circle (Debye ring), instead of distinct spots, because they are composed of crystallites with a size significantly smaller

DOI: 10.1021/acs.langmuir.6b03359
Langmuir 2016, 32, 12876−12884

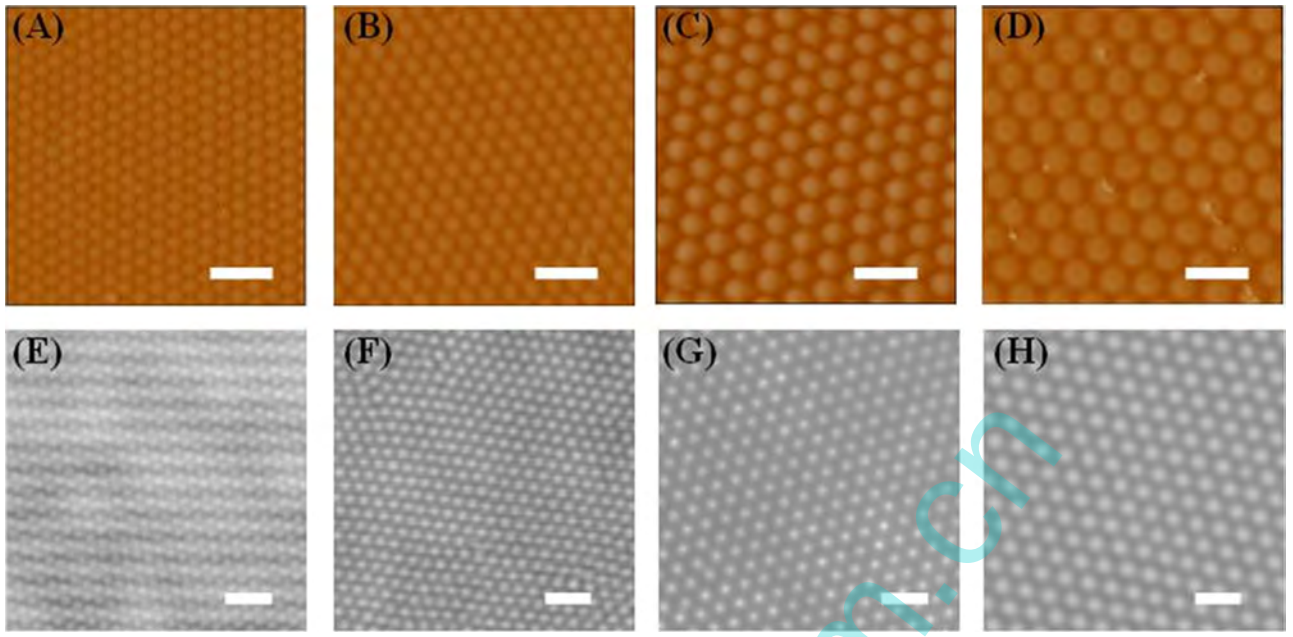

Figure 3. AFM (A–D) and optical microscopy images (E–H) of 2D CCs from 700 nm (A,E), 850 nm (B,F), 1030 nm (C,G), and 1430 nm microgels (D,H). The concentration of the microgel dispersions is 2.86, 3.20, 3.32, and 3.10 wt %, respectively. Scale bar: 2 μm.

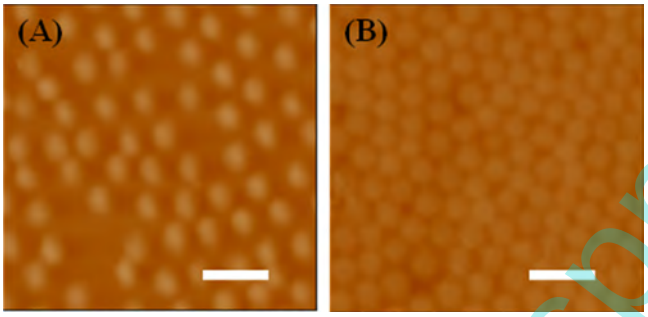

Figure 4. AFM images of 2D microgel arrays fabricated using a bare glass slide (without surface modification) (A) and amino-modified glass slide (B) as a substrate. Scale bar: 2 μm.

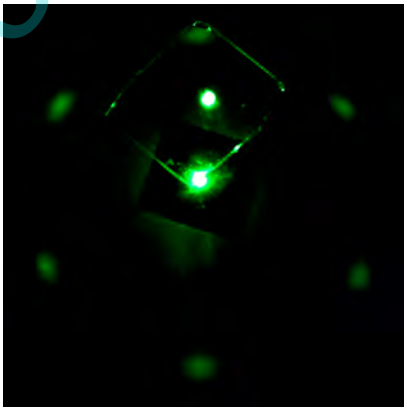

Figure 5. Diffraction pattern of normally incident laser beam transmitted through a 2D microgel CC. The size of the sample is 2 × 2 cm.

than the beam diameter, and the crystallites are randomly oriented.[58,59] By contrast, the 2D microgel CCs fabricated here display a diffraction pattern with six symmetrical spots (Figure 5), suggesting that the microgel particles in the illuminated area (~2 mm in diameter) are arranged perfectly into a hexagonal crystalline array.

To quantitatively characterize their ordering, the dimensionless pair correlation function, $g(r)$, was calculated. $g(r)$ is defined by the following equation

$$g(r) = \frac{1}{\langle\rho\rangle}\frac{\mathrm{d}n(r, r+\mathrm{d}r)}{\mathrm{d}a(r, r+\mathrm{d}r)} \quad (1)$$

where $\langle\rho\rangle$ is the average particle number density, a is the shell area, and $n(r,r + \mathrm{d}r)$ is the number of particles that lie within the shell considered.[6,60] The function describes the probability to find a particle at a distance r from a given particle in the 2D space. The peaks in the distribution indicate the preferred distances and are considered as a signature of order of the 2D array. As an example, Figure 6A compares $g(r)$ of a 2D CC with 700 nm microgel and the one calculated for a perfectly packed hexagonal array. $g(r)$ of the 2D microgel CC displays a series of peaks, suggesting the extension of structural order over a long distance. In addition, the positions of the peaks are coincident with those of the perfectly packed hexagonal array, confirming hexagonal packing of the particles.

The ratio of the full width at half maximum of the first peak in the Fourier transform (FT) of the function $g(r) - 1$, k, to that of a perfectly packed array, k_0, is another quantitative measure of ordering.[6,60] If the particles are perfectly packed, the ratio will be 1. It becomes larger with increasing disorder in the structure. Generally, a k/k_0 value less than 1.5 indicates a highly ordered structure, whereas a k/k_0 value larger than 1.5 indicates significant disordering.[6,60] For the same 2D microgel CC, the k/k_0 value was determined to be 1.16 (Figure 6B), suggesting a highly ordered structure. The k/k_0 value for 2D CCs from other microgels is also close to 1 (1.08, 1.21, and 1.34 for 2D CCs from 850, 1030, and 1430 nm microgels, respectively).

One advantage of the method is that the interparticle distance of the 2D microgel CCs can be tuned by the concentration of the microgel dispersion. As an example, Figure 7 shows the 2D arrays fabricated using different concentrations

DOI: 10.1021/acs.langmuir.6b03359
Langmuir 2016, 32, 12876–12884

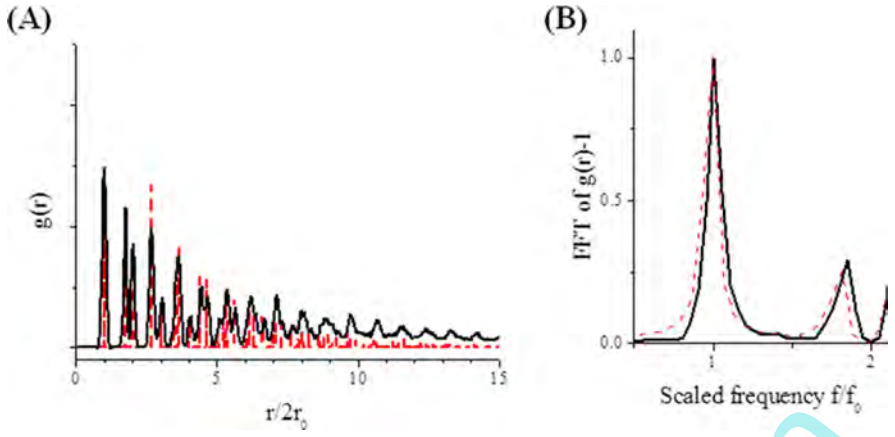

Figure 6. (A) Pair correlation function, $g(r)$, of the 2D CC from 700 nm microgel. Dashed vertical lines indicate the peaks of $g(r)$ of an ideal hexagonally packed monolayer generated numerically. (B) Single-sided power spectral FT of $g(r)$ compared with the FT of the corresponding perfectly ordered arrays. The power spectra were scaled to have identical maxima at $f/f_0 = 1.0$.[6]

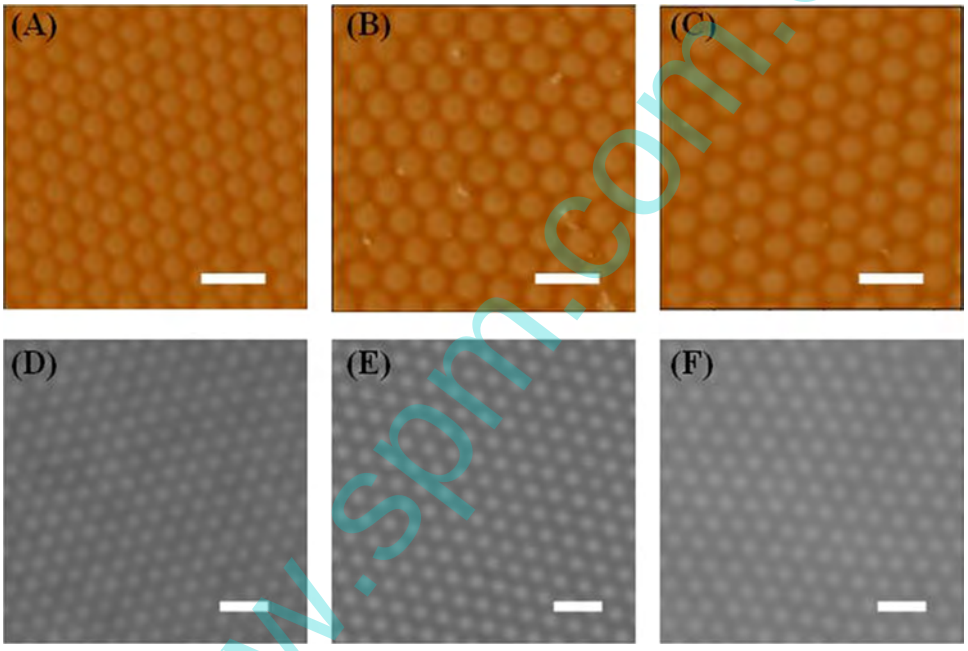

Figure 7. AFM (A–C) and optical microscopy images (D–F) of 2D CCs from 1430 nm microgel. Concentration of the microgel dispersion is 3.75 wt % (A,D), 3.10 wt % (B,E), and 2.85 wt % (C,F). The interparticle distance is ~1000 nm (A,D), ~1100 nm (B,E), and ~1200 nm (C,F). Scale bar: 2 μm.

of 1430 nm microgel. One can observe that the interparticle distance of the 2D arrays decreases with increasing dispersion concentration. By decreasing the dispersion concentration from 3.75 to 2.85 wt %, the interparticle distance increases from ~1000 to ~1200 nm. Previous studies have revealed that the crystallization of higher concentration dispersion will result in a 3D CC with a reduced interparticle distance.[35,39] When the first 111 plane of the 3D CC is fixed in situ on the substrate, a 2D array with a shorter interparticle distance will be obtained (Scheme 1).

Most of the existing methods can only produce 2D CCs with a relatively small size.[6,20] For example, Tsuji and Kawaguchi[26] fabricated 2D microgel CCs by air-drying a diluted microgel dispersion. The resulting colored array has a small size of only 0.36 cm^2. By contrast, the method developed here allows for the fabrication of large-area 2D CCs. As an example, Figure 8A shows the image of a 2D microgel CC fabricated on a glass slide

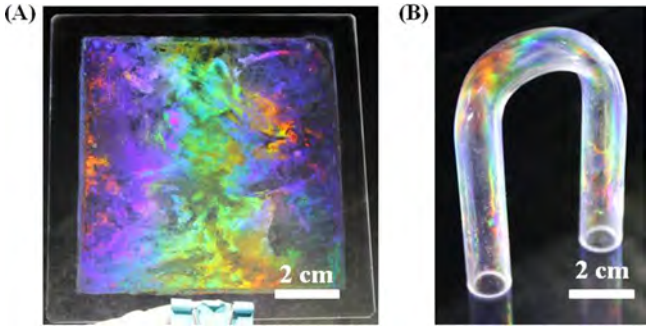

Figure 8. (A) Photograph of a 10 × 10 cm^2 glass slide on which a 2D microgel CC was fabricated. The area of the 2D array is ~64 cm^2. (B) Photograph of a U tube with 2D microgel CC fabricated on its inner wall.

DOI: 10.1021/acs.langmuir.6b03359
Langmuir 2016, 32, 12876–12884

with a size of 10 × 10 cm^2. The area of the resulting CC is ~64 cm^2. When illuminated with white light obliquely from behind, the 2D CC displays vivid diffraction colors, suggesting that the microgel particles were arranged into a highly ordered structure. As many previously reported 2D CCs, different parts of the array display different colors. This phenomenon can be explained by the different angles at which the individual part is illuminated.[6,58] A second reason for the different colors observed may be the polycrystalline nature of the array.[35] Fabrication of 2D microgel CCs with even larger size is possible because 3D microgel CCs of any size can be facilely assembled.[42]

Another limitation for most of the existing methods is that they can only use planar substrates. By contrast, the method developed here can use not only planar substrates but also nonplanar ones. To demonstrate this, the inner wall of a U-tube was first modified with APTES and then with 2,2-dimethylsuccinic anhydride. Concentrated microgel dispersion was then added and aged for 5 days. After removing the unbound microgel spheres and drying, the tube displays vivid diffraction colors when illuminated with white light obliquely from behind, suggesting that a crystalline array of microgel particles was successfully fabricated on the inner surface of the tube (Figure 8B).

Assembly of 2D CC on Other Substrates. Besides glass slides, quartz slides and silicon wafers, PET and PVC films were also used as a substrate for the fabrication of 2D microgel CCs. Like glass slides, quartz slides and silicon wafers were first treated with APTES and then with 2,2-dimethylsuccinic anhydride to make them charge-reversible. As an example, Figure S3 shows a photograph of a 2D CC fabricated on the silicon wafer. The size of the array is ~45 cm^2.

Unlike the rigid inorganic substrates, polymer films are flexible. To prepare charge-reversible polymer films, amino groups were first introduced. For this purpose, PET films were aminolyzed with 1,6-diaminohexane using a reported procedure,[47,48] whereas PVC films were aminated with ethylenediamine at 80 °C, according to Jayakrishnan et al.[49] Similarly, the surface amino groups were then protected by reaction with 2,2-dimethylsuccinic anhydride (Scheme S2). The surface-modified films were then used to fabricate a 2D microgel CC by assembling a 3D microgel CC on their surface. With the hydrolysis of the amide bonds and surface charge reversal, the first 111 plane of the 3D CC will be fixed in situ.

Figure 9A,B shows the photographs of 2D microgel CCs fabricated using PET and PVC films as a substrate. Like the 2D CCs fabricated on the glass slides (Figure 8A), these 2D CCs also display vivid diffraction colors, suggesting that the microgel particles formed a highly ordered structure. Figure 9C,D shows the AFM images of the 2D CCs, which clearly show that the microgel spheres were arranged into a hexagonal crystalline array. The size of the 2D CC is ~46 and ~42 cm^2, confirming again the ability of the method to fabricate large-area 2D CCs.

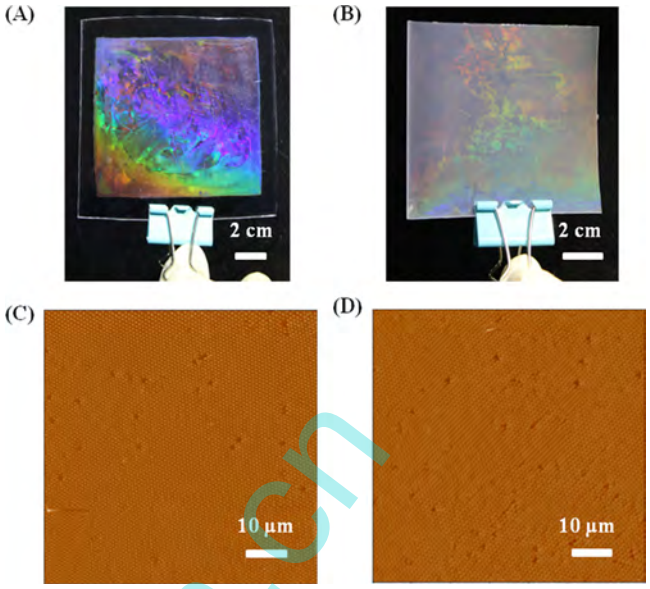

Figure 9. (A,B) Photographs of a PET film (A) and a PVC film (B) on which a 2D microgel CC was fabricated. (C,D) AFM images of the 2D microgel monolayer on the PET film (C) and on the PVC film (D).

CONCLUSIONS

In conclusion, we demonstrated that 2D microgel CCs could be simply fabricated by applying concentrated microgel dispersion on the charge-reversible substrate. The microgel spheres first self-assemble into a 3D CC. With the charge reversal of the substrate, the first 111 plane of the 3D assembly is fixed in situ on the substrate, leaving a high-quality 2D CC.

The charge-reversible substrates were prepared by first modifying with amino groups, followed by amidation with 2,2-dimethylsuccinic anhydride. As the amino groups were protected, they will not disturb the self-assembly of the microgel spheres. Meanwhile, as the resulting amide is hydrolyzable at low pH, the surface amino group will be regenerated. The surface charge of the substrate will change from negative to positive. As a result, the negatively charged microgel spheres will be fixed onto the substrate via electrostatic interaction.

Taking advantage of the high quality of 3D microgel CCs, the resulting 2D CCs also have a high degree of ordering. In addition, the method allows the fabrication of large-area 2D microgel CCs and the use of nonplanar substrates. Interparticle distance of the 2D array can be tuned by the concentration of the microgel dispersion. Various charge-reversible substrates, including both rigid and flexible ones, were successfully used for the fabrication of 2D microgel CCs, suggesting the universality of the method. We hope that the method will pave the way for the application of 2D microgel CCs, especially in surface patterning and chemical sensing.

ASSOCIATED CONTENT

Supporting Information

The Supporting Information is available free of charge on the ACS Publications website at DOI: 10.1021/acs.langmuir.6b03359.

Hydrodynamic diameter and zeta potential of the microgel spheres, photographs of 3D CC and 2D CC on silicon wafer, modification of silica particles, PET and PVC films (PDF)

AUTHOR INFORMATION

Corresponding Authors

*E-mail: yingguan@nankai.edu.cn (Y.G.).
*E-mail: yongjunzhang@nankai.edu.cn (Y.Z.).

ORCID

Yongjun Zhang: 0000-0002-1079-4137

DOI: 10.1021/acs.langmuir.6b03359
Langmuir 2016, 32, 12876−12884

Notes

The authors declare no competing financial interest.

■ ACKNOWLEDGMENTS

We thank financial support for this work from the National Natural Science Foundation of China (Grants nos 21274068, 21374048, and 51625302), the Tianjin Committee of Science and Technology (16JCZDJC32900), and PCSIRT program (IRT1257).

■ REFERENCES

(1) Zhang, J.; Li, Y.; Zhang, X.; Yang, B. Colloidal Self-Assembly Meets Nanofabrication: From Two-Dimensional Colloidal Crystals to Nanostructure Arrays. *Adv. Mater.* **2010**, *22*, 4249−4269.
(2) Ye, X.; Qi, L. Recent advances in fabrication of monolayer colloidal crystals and their inverse replicas. *Sci. China: Chem.* **2014**, *57*, 58−69.
(3) Yang, S.; Lei, Y. Recent progress on surface pattern fabrications based on monolayer colloidal crystal templates and related applications. *Nanoscale* **2011**, *3*, 2768−2782.
(4) Vogel, N.; Weiss, C. K.; Landfester, K. From soft to hard: The generation of functional and complex colloidal monolayers for nanolithography. *Soft Matter* **2012**, *8*, 4044−4061.
(5) Cong, H.; Yu, B.; Tang, J.; Li, Z.; Liu, X. Current status and future developments in preparation and application of colloidal crystals. *Chem. Soc. Rev.* **2013**, *42*, 7774−7800.
(6) Zhang, J.-T.; Wang, L.; Lamont, D. N.; Velankar, S. S.; Asher, S. A. Fabrication of Large-Area Two-Dimensional Colloidal Crystals. *Angew. Chem., Int. Ed.* **2012**, *51*, 6117−6120.
(7) Zhang, J.-T.; Wang, L.; Luo, J.; Tikhonov, A.; Kornienko, N.; Asher, S. A. 2-D Array Photonic Crystal Sensing Motif. *J. Am. Chem. Soc.* **2011**, *133*, 9152−9155.
(8) Men, D.; Zhang, H.; Hang, L.; Liu, D.; Li, X.; Cai, W.; Xiong, Q.; Li, Y. Optical sensor based on hydrogel films with 2D colloidal arrays attached on both the surfaces: Anti-curling performance and enhanced optical diffraction intensity. *J. Mater. Chem. C* **2015**, *3*, 3659−3665.
(9) Xue, F.; Meng, Z.; Wang, F.; Wang, Q.; Xue, M.; Xu, Z. A 2-D photonic crystal hydrogel for selective sensing of glucose. *J. Mater. Chem. A* **2014**, *2*, 9559−9565.
(10) Kargar, M.; Pruden, A.; Ducker, W. A. Preventing bacterial colonization using colloidal crystals. *J. Mater. Chem. B* **2014**, *2*, 5962−5971.
(11) Ye, R.; Ye, Y.-H.; Zhou, Z.; Xu, H. Gravity-Assisted Convective Assembly of Centimeter-Sized Uniform Two-Dimensional Colloidal Crystals. *Langmuir* **2013**, *29*, 1796−1801.
(12) Sun, X.; Li, Y.; Zhang, T. H.; Ma, Y.-q.; Zhang, Z. Fabrication of Large Two-Dimensional Colloidal Crystals via Self-Assembly in an Attractive Force Gradient. *Langmuir* **2013**, *29*, 7216−7220.
(13) Ng, E. C. H.; Chin, K. M.; Wong, C. C. Controlling Inplane Orientation of a Monolayer Colloidal Crystal by Meniscus Pinning. *Langmuir* **2011**, *27*, 2244−2249.
(14) Born, P.; Munoz, A.; Cavelius, C.; Kraus, T. Crystallization Mechanisms in Convective Particle Assembly. *Langmuir* **2012**, *28*, 8300−8308.
(15) Xue, F.; Asher, S. A.; Meng, Z.; Wang, F.; Lu, W.; Xue, M.; Qi, F. Two-dimensional colloidal crystal heterostructures. *RSC Adv.* **2015**, *5*, 18939−18944.
(16) Xue, F.; Meng, Z.; Qi, F.; Xue, M.; Qiu, L. Preparation of free-standing two-dimensional colloidal crystal arrays. *Colloid Polym. Sci.* **2016**, *294*, 479−482.
(17) Yang, H.; Gozubenli, N.; Fang, Y.; Jiang, P. Generalized Fabrication of Monolayer Nonclose-Packed Colloidal Crystals with Tunable Lattice Spacing. *Langmuir* **2013**, *29*, 7674−7681.
(18) Jiang, P.; McFarland, M. J. Large-Scale Fabrication of Wafer-Size Colloidal Crystals, Macroporous Polymers and Nanocomposites by Spin-Coating. *J. Am. Chem. Soc.* **2004**, *126*, 13778−13786.
(19) Zhang, G.; Wang, D.; Gu, Z.-Z.; Hartmann, J.; Möhwald, H. Two-Dimensional Non-Close-Packing Arrays Derived from Self-Assembly of Biomineralized Hydrogel Spheres and Their Patterning Applications. *Chem. Mater.* **2005**, *17*, 5268−5274.
(20) Horecha, M.; Senkovskyy, V.; Synytska, A.; Stamm, M.; Chervanyov, A. I.; Kiriy, A. Ordered surface structures from PNIPAM-based loosely packed microgel particles. *Soft Matter* **2010**, *6*, 5980−5992.
(21) Rey, B. M.; Elnathan, R.; Ditcovski, R.; Geisel, K.; Zanini, M.; Fernandez-Rodriguez, M.-A.; Naik, V. V.; Frutiger, A.; Richtering, W.; Ellenbogen, T.; Voelcker, N. H.; Isa, L. Fully Tunable Silicon Nanowire Arrays Fabricated by Soft Nanoparticle Templating. *Nano Lett.* **2016**, *16*, 157−163.
(22) Guan, Y.; Zhang, Y. PNIPAM microgels for biomedical applications: From dispersed particles to 3D assemblies. *Soft Matter* **2011**, *7*, 6375−6384.
(23) Pelton, R. H.; Chibante, P. Preparation of aqueous latices with N-isopropylacrylamide. *Colloids Surf.* **1986**, *20*, 247−256.
(24) Xia, Y.; He, X.; Cao, M.; Wang, X.; Sun, Y.; He, H.; Xu, H.; Lu, J. R. Self-Assembled Two-Dimensional Thermoresponsive Microgel Arrays for Cell Growth/Detachment Control. *Biomacromolecules* **2014**, *15*, 4021−4031.
(25) Schmidt, S.; Hellweg, T.; von Klitzing, R. Packing Density Control in P(NIPAM-co-AAc) Microgel Monolayers: Effect of Surface Charge, pH, and Preparation Technique. *Langmuir* **2008**, *24*, 12595−12602.
(26) Tsuji, S.; Kawaguchi, H. Colored thin films prepared from hydrogel microspheres. *Langmuir* **2005**, *21*, 8439−8442.
(27) Lu, Y.; Drechsler, M. Charge-Induced Self-Assembly of 2-Dimensional Thermosensitive Microgel Particle Patterns. *Langmuir* **2009**, *25*, 13100−13105.
(28) Horigome, K.; Suzuki, D. Drying Mechanism of Poly(*N*-isopropylacrylamide) Microgel Dispersions. *Langmuir* **2012**, *28*, 12962−12970.
(29) Quint, S. B.; Pacholski, C. Extraordinary long range order in self-healing non-close packed 2D arrays. *Soft Matter* **2011**, *7*, 3735−3738.
(30) Geisel, K.; Richtering, W.; Isa, L. Highly ordered 2D microgel arrays: Compression versus self-assembly. *Soft Matter* **2014**, *10*, 7968−7976.
(31) Vogel, N.; Fernández-López, C.; Pérez-Juste, J.; Liz-Marzán, L. M.; Landfester, K.; Weiss, C. K. Ordered Arrays of Gold Nanostructures from Interfacially Assembled Au@PNIPAM Hybrid Nanoparticles. *Langmuir* **2012**, *28*, 8985−8993.
(32) Li, X.; Weng, J.; Guan, Y.; Zhang, Y. Fabrication of large-area two-dimensional microgel colloidal crystals via interfacial thiol−ene click reaction. *Langmuir* **2016**, *32*, 3977−3982.
(33) Weng, J.; Li, X.; Guan, Y.; Zhu, X. X.; Zhang, Y. Large-area 2D microgel colloidal crystals fabricated via benzophenone-based photochemical reaction. *RSC Adv.* **2016**, *6*, 82006−82013.
(34) Hu, Z.; Huang, G. A new route to crystalline hydrogels, guided by a phase diagram. *Angew. Chem., Int. Ed.* **2003**, *42*, 4799−4802.
(35) Debord, J. D.; Eustis, S.; Debord, S. B.; Lofye, M. T.; Lyon, L. A. Color-tunable colloidal crystals from soft hydrogel nanoparticles. *Adv. Mater.* **2002**, *14*, 658−662.
(36) Chen, M.; Zhou, L.; Guan, Y.; Zhang, Y. Polymerized Microgel Colloidal Crystals: Photonic Hydrogels with Tunable Band Gaps and Fast Response Rate. *Angew. Chem., Int. Ed.* **2013**, *52*, 9961−9965.
(37) Liu, Y.; Guan, Y.; Zhang, Y. Facile Assembly of 3D Binary Colloidal Crystals from Soft Microgel Spheres. *Macromol. Rapid Commun.* **2014**, *35*, 630−634.
(38) Chen, M.; Zhang, Y.; Jia, S.; Zhou, L.; Guan, Y.; Zhang, Y. Photonic Crystals with a Reversibly Inducible and Erasable Defect State Using External Stimuli. *Angew. Chem., Int. Ed.* **2015**, *54*, 9257−9261.
(39) Gao, J.; Hu, Z. Optical properties of *N*-isopropylacrylamide microgel spheres in water. *Langmuir* **2002**, *18*, 1360−1367.
(40) Debord, J. D.; Lyon, L. A. Thermoresponsive photonic crystals. *J. Phys. Chem. B* **2000**, *104*, 6327−6331.
(41) Iyer, A. S. J.; Lyon, L. A. Self-Healing Colloidal Crystals. *Angew. Chem., Int. Ed.* **2009**, *48*, 4562−4566.

DOI: 10.1021/acs.langmuir.6b03359
Langmuir 2016, 32, 12876−12884

(42) Hellweg, T. Towards Large-Scale Photonic Crystals with Tuneable Bandgaps. *Angew. Chem., Int. Ed.* **2009**, *48*, 6777−6778.
(43) Jones, C. D.; Lyon, L. A. Synthesis and characterization of multiresponsive core−shell microgels. *Macromolecules* **2000**, *33*, 8301−8306.
(44) Mahalingam, V.; Onclin, S.; Péter, M.; Ravoo, B. J.; Huskens, J.; Reinhoudt, D. N. Directed Self-Assembly of Functionalized Silica Nanoparticles on Molecular Printboards through Multivalent Supramolecular Interactions. *Langmuir* **2004**, *20*, 11756−11762.
(45) Howarter, J. A.; Youngblood, J. P. Optimization of silica silanization by 3-aminopropyltriethoxysilane. *Langmuir* **2006**, *22*, 11142−11147.
(46) Kim, J.; Cho, J.; Seidler, P. M.; Kurland, N. E.; Yadavalli, V. K. Investigations of Chemical Modifications of Amino-Terminated Organic Films on Silicon Substrates and Controlled Protein Immobilization. *Langmuir* **2010**, *26*, 2599−2608.
(47) Avadanei, M.; Drobota, M.; Stoica, I.; Rusu, E.; Barboiu, V. Surface morphology and amide concentration depth profile of aminolyzed poly(ethylene terephthalate) films. *J. Polym. Sci., Part A: Polym. Chem.* **2010**, *48*, 5456−5467.
(48) He, D.; Ulbricht, M. Synergist Immobilization Method for Photo-Grafting: Factors Affecting Surface Selectivity. *Macromol. Chem. Phys.* **2007**, *208*, 1582−1591.
(49) Balakrishnan, B.; Kumar, D. S.; Yoshida, Y.; Jayakrishnan, A. Chemical modification of poly(vinyl chloride) resin using poly(ethylene glycol) to improve blood compatibility. *Biomaterials* **2005**, *26*, 3495−3502.
(50) Xu, P.; Van Kirk, E. A.; Zhan, Y.; Murdoch, W. J.; Radosz, M.; Shen, Y. Targeted Charge-Reversal Nanoparticles for Nuclear Drug Delivery. *Angew. Chem., Int. Ed.* **2007**, *46*, 4999−5002.
(51) Lee, Y.; Fukushima, S.; Bae, Y.; Hiki, S.; Ishii, T.; Kataoka, K. A Protein Nanocarrier from Charge-Conversion Polymer in Response to Endosomal pH. *J. Am. Chem. Soc.* **2007**, *129*, 5362−5363.
(52) Zhou, Z.; Shen, Y.; Tang, J.; Fan, M.; Van Kirk, E. A.; Murdoch, W. J.; Radosz, M. Charge-Reversal Drug Conjugate for Targeted Cancer Cell Nuclear Drug Delivery. *Adv. Funct. Mater.* **2009**, *19*, 3580−3589.
(53) Du, J.-Z.; Sun, T.-M.; Song, W.-J.; Wu, J.; Wang, J. A Tumor-Acidity-Activated Charge-Conversional Nanogel as an Intelligent Vehicle for Promoted Tumoral-Cell Uptake and Drug Delivery. *Angew. Chem., Int. Ed.* **2010**, *122*, 3703−3708.
(54) Zhou, Z.; Shen, Y.; Tang, J.; Jin, E.; Ma, X.; Sun, Q.; Zhang, B.; Van Kirk, E. A.; Murdoch, W. J. Linear polyethyleneimine-based charge-reversal nanoparticles for nuclear-targeted drug delivery. *J. Mater. Chem.* **2011**, *21*, 19114−19123.
(55) Brijitta, J.; Tata, B. V. R.; Joshi, R. G.; Kaliyappan, T. Random hcp and fcc structures in thermoresponsive microgel crystals. *J. Chem. Phys.* **2009**, *131*, 074904−074908.
(56) Debord, S. B.; Lyon, L. A. Influence of particle volume fraction on packing in responsive hydrogel colloidal crystals. *J. Phys. Chem. B* **2003**, *107*, 2927−2932.
(57) Alsayed, A. M.; Islam, M. F.; Zhang, J.; Collings, P. J.; Yodh, A. G. Premelting at defects within bulk colloidal crystals. *Science* **2005**, *309*, 1207−1210.
(58) Prevo, B. G.; Velev, O. D. Controlled, Rapid Deposition of Structured Coatings from Micro- and Nanoparticle Suspensions. *Langmuir* **2004**, *20*, 2099−2107.
(59) Zhang, J.-T.; Chao, X.; Liu, X.; Asher, S. A. Two-dimensional array Debye ring diffraction protein recognition sensing. *Chem. Commun.* **2013**, *49*, 6337−6339.
(60) Rengarajan, R.; Mittleman, D.; Rich, C.; Colvin, V. Effect of disorder on the optical properties of colloidal crystals. *Phys. Rev. E: Stat., Nonlinear, Soft Matter Phys.* **2005**, *71*, 016615.

DOI: 10.1021/acs.langmuir.6b03359
Langmuir 2016, 32, 12876−12884